On the Lateral Entrainment Instability in the Inner Core Region of Tropical Cyclones

Ping Zhu[1], Jun A. Zhang[2,3], and Frank D. Marks[3]

[1]Department of Earth and Environment, Florida International University

[2]Cooperative Institute for Marine and Atmospheric Studies, University of Miami

[3]Hurricane Research Division, Atlantic Oceanographic and Meteorological Laboratory, NOAA

Corresponding author: Ping Zhu (zhup@fiu.edu), 11200 SW 8th ST, Miami, FL, 33199.

Key Points:

- Lateral entrainment of air from the moat region into eyewall and rainbands of a tropical cyclone satisfies the instability criterion.
- Positive buoyancy flux induced by the entrainment is an important source of turbulent kinetic energy for the eyewall and rainband clouds.
- Lateral entrainment instability should be included in turbulent mixing parameterizations in tropical cyclone forecast models.

Abstract

Entrainment of dry moat air with low equivalent potential temperature laterally into the eyewall and rainbands is a unique turbulent process in the inner-core region of a tropical cyclone (TC). By analyzing in-situ aircraft measurements collected by the reconnaissance flights that penetrated the eyewalls and rainbands of Hurricanes Rita (2005), Patricia (2015), Harvey (2017), and Michael (2018), as well as numerical simulations of Hurricanes Patricia (2015) and Michael (2018), we show that the moat air entrained into the eyewall and rainbands meets the instability criterion, and therefore, sinks unstably as a convective downdraft. The resultant positive buoyancy fluxes are an important source for the turbulent kinetic energy (TKE) in the eyewall and rainband clouds. This mechanism of TKE generation via lateral entrainment instability should be included in the TKE-type turbulent mixing schemes for a better representation of turbulent transport processes in numerical forecasts of TCs.

Plain Language Summary

Turbulence is commonly regarded as a chaotic flow feature pertaining to the planetary boundary layer (PBL). In the inner core of a tropical cyclone (TC), however, turbulence can also be generated in the eyewall and rainbands above the PBL by cloud processes. The turbulence at the edge of the eyewall/rainbands not only experiences the large lateral thermodynamic contrasts across the interface between clouds and moat but also entrains moat air into clouds. Previous studies suggest that under certain conditions the entrained air into the clouds can sink unstably as convective downdrafts, leading to the generation of turbulent kinetic energy (TKE) in the clouds. By analyzing in-situ aircraft measurements collected during the reconnaissance flights that penetrated the eyewalls and rainbands of Hurricanes Rita (2005), Patricia (2015), Harvey (2017), and Michael (2018), as well as numerical simulations of Patricia (2015) and Michael (2018), this study shows that the moat air entrained into the eyewall and rainbands meets the instability criterion. An estimate of the entrainment buoyancy fluxes suggests that the lateral entrainment instability is an important source of TKE in the eyewall and rainbands, and thus, it needs to be included in the TKE-type turbulence schemes used in numerical forecasts of TCs.

1 Introduction

The entrainment instability at the top of clouds was first recognized by Lilly (1968) and later well documented by Deardorff (1980) and Randall (1980). Under cloud free conditions, entrainment of air from the free atmosphere above into the turbulent boundary layer tends to destroy the turbulent kinetic energy (TKE) since the buoyancy force acts to oppose the vertical motions in the boundary layer. For the boundary layer topped by stratocumulus clouds, however, the evaporative cooling of the unsaturated free atmosphere air that has been entrained into clouds may cause the entrained air to sink unstably as a convective downdraft owing to its negative buoyancy. This process leads to the generation of TKE in the stratocumulus layer. Deardorff (1980) showed that the entrainment buoyancy flux, $(\overline{w'\theta_v'})_{ctp\_e}$, may be written as a function of the jumps of conserved thermodynamic variables across the top of the stratocumulus layer as,

$$(\overline{w'\theta_v'})_{ctp\_e} = w_{ctp\_e}\left(-\alpha\Delta_{ctp}\theta_e + \bar{\theta}\Delta_{ctp}q_t\right), \quad (1)$$

where θ_e is the equivalent potential temperature defined as $\theta_e = \theta(1 + \frac{L}{c_pT}q)$; T is temperature; θ is potential temperature; q is water vapor mixing ratio; L is specific latent heat of vaporization; c_p is the specific heat of dry air at the constant pressure; q_t is total water mixing ratio; θ_v is virtual potential temperature; w_{ctp_e} is the cloud-top entrainment velocity; α is a theoretical coefficient resulting from the derivation involving with the moist thermodynamics, and it has a value near 0.5, but may vary from 1/3 to 2/3 depending on specific conditions; Δ_{ctp} is defined as the difference of the above-cloud value minus the in-cloud value; and overbar and prime indicate the mean and perturbations away from the mean, respectively. Since w_{ctp_e} is positive and $\Delta_{ctp}q_t$ is negative, if $\Delta_{ctp}\theta_e$ is more negative than a criterion, $\Delta_{ctp}\theta_e < (\Delta_{ctp}\theta_e)_{crit} = \bar{\theta}\Delta_{ctp}q_t/\alpha$, it will, then, result in positive entrainment buoyancy fluxes, $(\overline{w'\theta_v'})_{ctp\_e} > 0$, leading to the generation of TKE in the stratocumulus layer. This is known as the cloud top entrainment instability and has been identified as an important mechanism for generating TKE in the clouds to maintain the stratocumulus layer.

Unlike the shallow-cloud topped boundary layer that is cleanly separated from the dry free atmosphere above by a capping inversion, observations show that in the eyewall and rainbands of a tropical cyclone (TC) large TKEs extend all the way to the upper troposphere from the boundary layer (e.g., Marks et al. 2008; Lorsolo et al. 2010, Zhang & Montgomery 2012, and Zhu et al. 2019) with no physical interface, such as an inversion, separating the turbulence generated by boundary layer processes and cloud processes aloft. Thus, cloud top entrainment instability associated with the shallow stratocumulus does not exist or is negligible in the TC inner-core region. However, turbulence generated in the eyewall and rainbands experiences a large lateral thermodynamic contrast across the interface between the eyewall/rainbands and moat. As an illustration, Figure 1 shows a height-radius distribution of the simulated total water mixing ratio and velocity vectors at the outer edge of the eyewall from a large eddy simulation (LES) of Hurricane Isabel (2003) given by Li et al. (2022). There are two well-defined large overturning eddy circulations in the scene. One is in the boundary layer and the other is in the mid troposphere at the cloud edge indicated by the thick black arrows. In both cases, turbulent eddies not only experience drastic lateral contrasts across the edge of the eyewall, but also entrain the dry and low θ_e air from the moat region laterally into the eyewall. Following the entrainment instability requirement (Deardorff 1980), if the lateral entrainment of the low θ_e moat air into the eyewall or rainbands meets the instability criterion, i.e.,

$$\Delta_{lat}\theta_e < (\Delta_{lat}\theta_e)_{crit} = \bar{\theta}\Delta_{lat}q_t/\alpha, \quad (2)$$

where Δ_{lat} refers to the lateral difference of the moat-air value minus the in-cloud value, then, lateral entrainment instability can occur, resulting in positive lateral entrainment buoyancy fluxes. This positive buoyancy flux can in turn serve as an important source for TKE generation in the eyewall and rainbands via buoyancy production of TKE (Stull 1988).

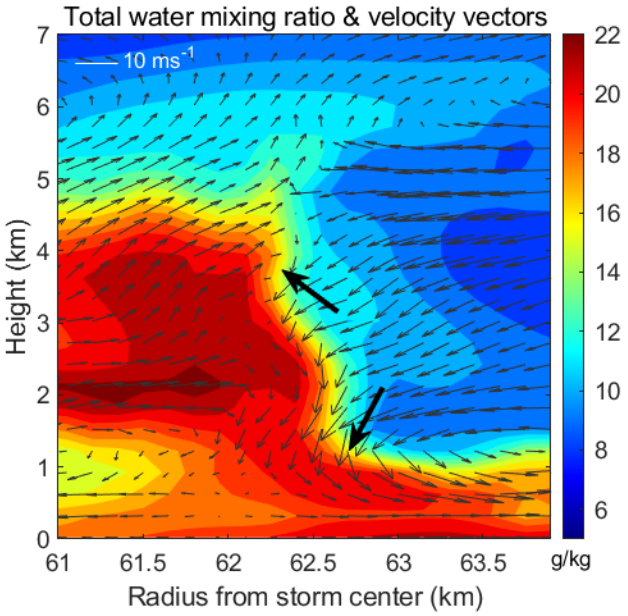

Figure 1: Height-radius distribution of total water mixing ratio (shading, g/kg) overlapped with the wind vectors associated with vertical velocity and radial flow near the outer edge of the eyewall from a large eddy simulation of Hurricane Isabel (2003) documented by Li et al. (2022). To clearly show the overturning eddy circulations, the mean radial flow over the area has been removed. Two thick dark arrows indicate the overturning turbulent eddy circulations in the scene.

Therefore, the main objective of this study is to verify if the lateral entrainment in the TC inner-core region satisfies the instability criterion stated above using both observations and numerical simulations. The importance and potential application of this TKE generation mechanism in eyewall and rainband clouds via lateral entrainment instability to the TKE type of turbulent mixing parameterizations used in TC forecast models are then discussed.

2 Evidences of lateral entrainment instability in TC inner core

To evaluate if the moat air laterally entrained into the eyewall and rainband clouds meets the instability criterion and is able to sink unstably as a convective downdraft, we examined the in-situ aircraft data collected during the Hurricane Research Division (HRD) reconnaissance flights that penetrated the eyewall and rainbands of Hurricanes Rita (2005), Patricia (2015), Harvey (2017), and Michael (2018) in total 113 radial legs. As an illustration, Figure 2 shows the 8 flight routes into Michael (2018) and the radial profiles of relative humidity, water vapor mixing ratio, equivalent potential temperature θ_e, and wind speed as a function of the distance from the storm center (i.e., radius) at approximately 750 hPa altitude from one of these legs that penetrated into Michael (2018). Details of the radial leg data from the HRD reconnaissance flights are provided in the supporting information file (S1). Since the flights do not have cloud measurements, we infer the locations of eyewall and rainbands as the radii where relative humidities are close to or exceed 1 as shown in Figs. 2b – 2e. We tested several values of relative humidity for saturation from 93% to 97%. It only shows a marginal effect on the analysis results. Therefore, in this paper the eyewall and rainbands in the radial legs are identified wherever the relative humidity exceeds 94%. The eyewall is, then, defined to be the region closest to the

maximum wind speed. The radial profile shown in Fig. 2d clearly show that the moat air in-between eyewall and rainbands has a lower θ_e than the saturated air in the eyewall and rainbands.

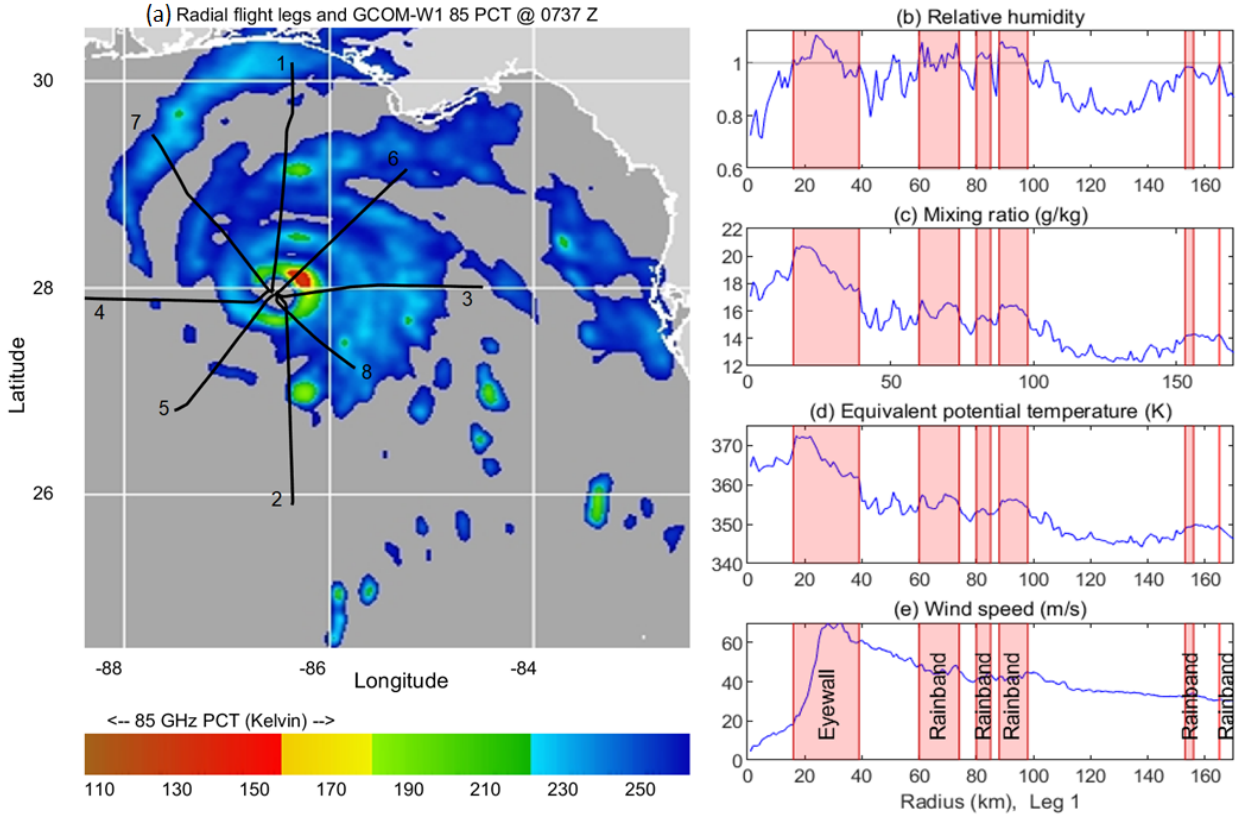

Figure 2: (a): Selected flights that penetrated into the eyewall and rainbands of Hurricane Michael (2018). (b) – (e): Radial profiles of relative humidity, water vapor mixing ratio, equivalent potential temperature, and wind speed as a function of radii from the storm center at ~ 750 hPa respectively from one of the flight legs.

We then estimate the difference of θ_e and mixing ratio between the identified unsaturated moat region and saturated eyewall and rainbands as follows. Since the radial resolution of the flight data is ~100 – 150 m, we average twenty observation points (~ 2 – 3 km) just inside and outside of the identified eyewall and rainbands to represent the mean thermodynamic properties of cloudy and moat air in the lateral entrainment, and then, calculate their differences between the moat and saturated eyewall and rainbands to examine if the entrained moat air into the eyewall and rainbands meets the instability criterion. Figure 3 shows the estimated $\Delta\theta_e$ against the instability criterion $\bar{\theta}\Delta q/\alpha$ for all edges between the identified eyewalls/rainbands and moats of the 50 radial flight legs into Rita (2005), 7 legs into Patricia (2015), 22 legs into Harvey (2017), and 34 legs into Michael (2018). Most (>95%) of the estimates fall clearly in the unstable regime! It should be pointed out that due to the lack of hydrometeor measurements in the aircraft data we have to replace the total water mixing ratio with the water vapor mixing ratio when calculating the instability criterion. Therefore, the actual value of $\bar{\theta}\Delta q/\alpha$ should be slightly more negative if the total water mixing ratio q_t were used. However, even if the hydrometeor mixing ratios were available and included in the calculation, the majority of the data points should still fall in the unstable regime, indicating that the moat air that is entrained laterally into eyewall and

rainband clouds has sufficiently low θ_e to meet the instability criterion and sinks unstably due to its own negative buoyancy. It should be noted that the above analysis only shows an entrainment instability potential. It remains unknown what percentage of moat air is actually entrained into the eyewall and rainband clouds by turbulence. This issue needs to be further investigated using relevant high-resolution observations and LESs.

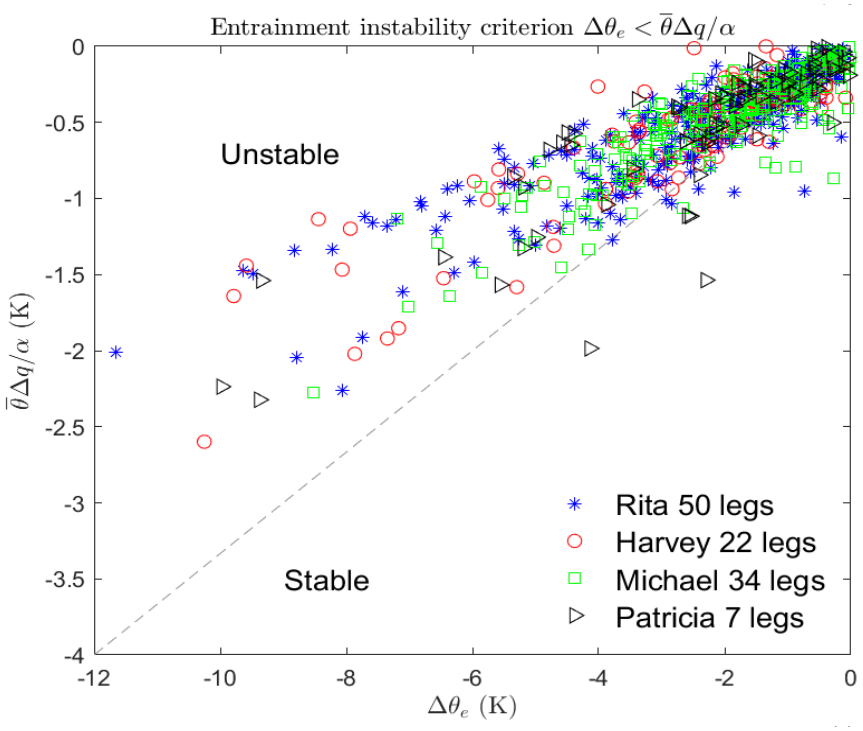

Figure 3: Equivalent potential temperature jumps across the identified eyewall/rainbands and moat, $\Delta\theta_e$, as a function of the corresponding $\bar{\theta}\Delta q/\alpha$ for 50 flight legs into Rita (2005), 7 legs into Patricia (2015), 22 legs into Harvey (2017), and 34 legs into Michael (2018) where Δ is defined as the difference of moat-air value minus in-cloud value.

To further evaluate the lateral entrainment instability in the TC inner core, we examined the numerical simulations of Hurricane Michael (2018) by the global-nested version of Hurricane Analysis and Forecast System (HAFS-globalnest, Zhu et al. 2021) and Hurricane Patricia (2015) by the Hurricane Weather Research and Forecasting (HWRF) model version 3.9a. Details of the numerical simulations are provided in the Supporting Information (S2). Figure 4 shows two arbitrary snapshots of the thermodynamic state of the simulated Michael (2018) and Patricia (2015) during their rapid intensification periods. Three consecutive grid points just inside, at, and outside of the outer edge of the eyewall are randomly selected whose locations with respect to the eyewall are shown in Figs. 4a and 4b, respectively. The distance between the grid points is approximately 1.22 km for HWRF since it was configured at the grid resolution of 0.011 degree, and 3 km for HAFS. Figures 4c – 4f show the vertical profiles of θ_e and q_t at these three grid points in the two simulations, respectively. We, then, evaluated the entrainment instability across the edge of the eyewall by calculating the instability parameter $\Delta_{lat}\theta_e - \bar{\theta}\Delta_{lat}q_t/\alpha$ using various combinations of the differences between the three grid points: green minus red, red minus black, and green minus black, respectively. The results (Figs. 4g and 4h) clearly show that $\Delta\theta_e$ is more negative than the instability criterion throughout the vertical column in both simulations, indicating that the entrained low θ_e moat air into the eyewall meets the instability criterion and thus will sink spontaneously due to its own negative buoyancy to generate TKE in

the eyewall. Note that we have examined the lateral entrainment instability criterion at various locations along the edge of eyewall with respect to down/up wind shear. All potential entrainments consistently meet the thermodynamic instability criterion. However, dynamically it remains unknown which quadrant of the eyewall with respect to wind shear is preferred for lateral entrainment, and this issue needs to be further investigated.

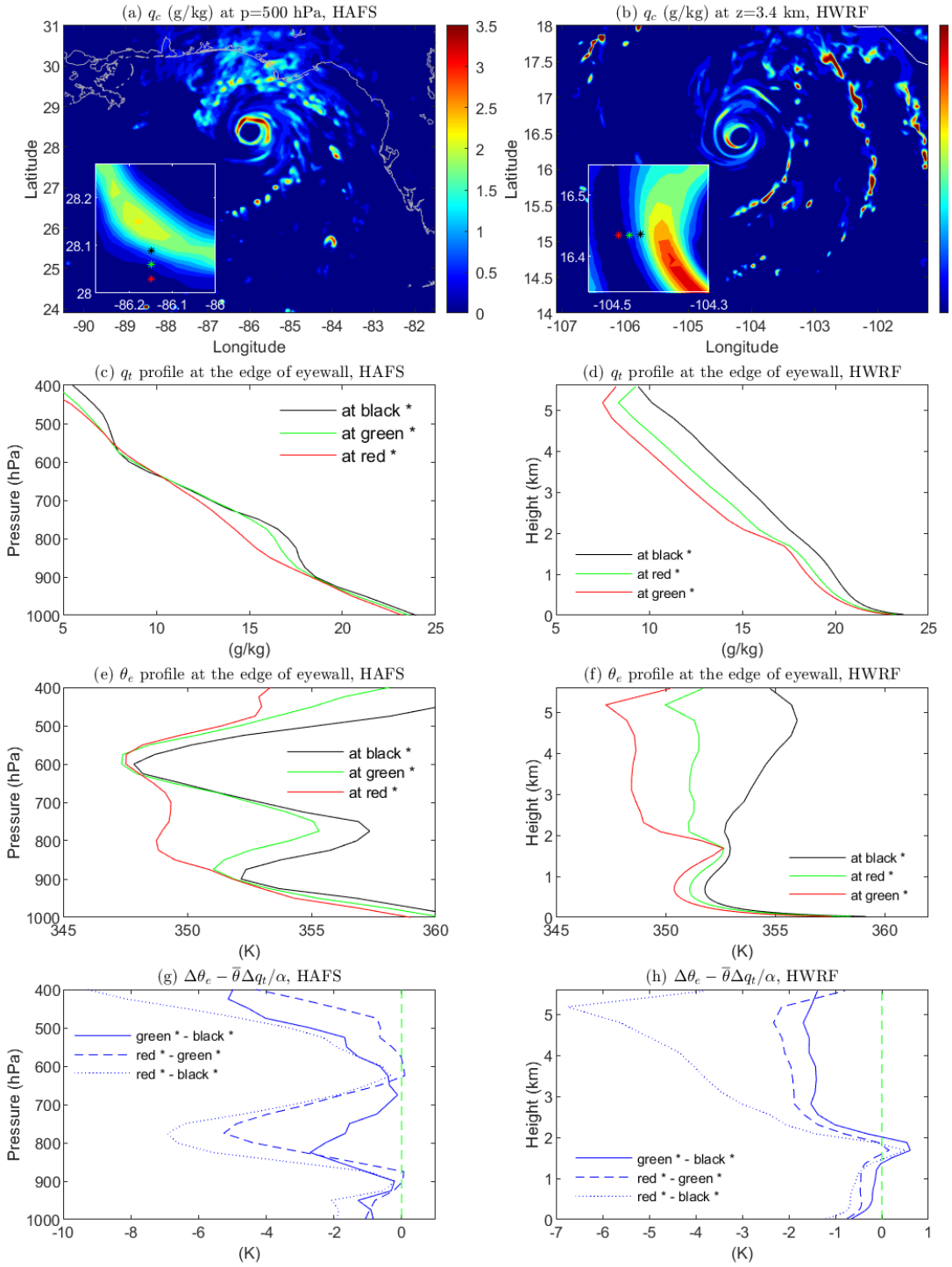

Figure 4: (a) and (b): Simulated hydrometeor mixing ratio at the altitude of 500 hPa and 3.4 km at an arbitrary time during the rapid intensification of Michael (2018) by HAFS and Patricia (2015) by HWRF, respectively. The inlaid panel shows the zoom-in view of the eyewall. Red, green, and black stars indicate the grid points in the vicinity of the eyewall to be analyzed. (c) and (f): vertical profiles of q_t and θ_e at the red, green, and black grid points, respectively. (g) and (h): Instability parameter calculated using different jumps between green and black grid points, red and green grid points, and red and black grid points, respectively.

3 Conclusion and discussion

Airborne radar observations show that large TKEs are generated in the eyewalls and rainbands by cloud processes aloft (e.g., Marks et al. 2008; Lorsolo et al. 2010, Zhang and Montgomery 2012, and Zhu et al. 2019). The resultant turbulent transport above the boundary layer plays an important role in the intensification of TCs (Zhu et al, 2019, 2021). In this study, by analyzing the in-situ aircraft data collected during the reconnaissance flight that penetrated the eyewall and rainbands of Hurricanes Rita (2005), Patricia (2015), Harvey (2017), and Michael (2018), as well as numerical simulations of Michael (2018) by HAFS and Patricia (2015) by HWRF, we show that the moat air if entrained into the eyewalls and rainbands will meet the instability criterion, leading to the potential unstable convective downdraft. The importance of this mechanism of TKE generation in the eyewall and rainbands via lateral entrainment instability may be inferred from an estimation of the resultant entrainment buoyancy fluxes. Following Eq. (1), the buoyancy fluxes induced by the lateral entrainment of moat air into the eyewalls and rainbands may be written as, $\rho c_p v_{lat}(-\alpha\Delta_{lat}\theta_e + \bar{\theta}\Delta_{lat}q_t)$, where ρ is the air density and v_{lat} is the lateral entrainment velocity. Although to date we have little knowledge on the lateral entrainment velocity in the TC inner core between the moat and convection, a lateral entrainment velocity of 0.3 m/s for the entrainment into convective thermals was previously derived from the comprehensive lidar and aircraft measurements (Crum et al. 1987). Based on the in-situ aircraft measurements (Fig. 3) and numerical simulations (Figs. 4g and 4 h), it is reasonable to assume the thermodynamic jump across the edge of eyewall and rainband clouds to be in a range $-\alpha\Delta_{lat}\theta_e + \bar{\theta}\Delta_{lat}q_t = [1-4]K$, further taking $v_{lat} = [0.1-\ 0.4]m/s$ based on the available observations (Crum et al. 1987), then, the entrainment buoyancy fluxes would be in a range of $[100-1600]\frac{W}{m^2}$, suggesting that the lateral entrainment instability should be one of the important mechanisms for generating TKEs in the eyewall and rainband clouds via TKE buoyancy production (Stull 1988).

The TKE-type turbulent mixing schemes now have been adopted in many research and operational models used for predicting TCs, such as, the Eddy-Diffusivity-Mass-Flux (EDMF) TKE scheme (Han and Bretherton 2019) used in the HAFS, a multi-scale Unified Forecast System (UFS) operational model and data assimilation package capable of providing analyses and forecasts of the inner core structure of TCs out to 7 days. The TKE schemes are attractive because they can provide a representation of turbulent transport induced by both the boundary-layer processes and cloud processes aloft in a unified manner regardless of the boundary layer height, provided that the buoyancy production, shear production, transport, and dissipation of TKE in a TKE budget equation can be correctly determined. This feature of a TKE scheme is particularly important in the TC inner core since the boundary layer becomes ill-defined as air approaches the eyewall and is pulled up into the active convection (Shapiro 1983; Smith et al. 2008, Smith and Montgomery 2010; Zhang et al. 2011). In the eyewalls and rainbands, buoyancy

production is an important source of TKE generation. The result presented in this study indicates that the lateral entrainment instability is an important physical process that needs to be included in the calculation of buoyancy production of TKE in numerical forecasts of TCs. Moreover, the lateral entrainment of moat air into the convective eyewalls and rainbands is a process that links horizontal and vertical turbulent mixing in the TC inner core. The positive lateral entrainment buoyancy flux promotes the TKE generation in the eyewall, which ensue enhances the lateral entrainment instability as more low-θ_e air in the moat is entrained into the eyewall. This positive feedback between the TKE generation in the eyewall clouds and lateral entrainment instability is unique for turbulence development and transport in the TC inner-core region, and thus, it must be represented realistically in numerical models for predicting TCs. We believe that the inclusion of lateral entrainment instability in model turbulent mixing schemes could address some of the issues regarding turbulence parameterization in TC simulations and correct prediction of RI raised by some recent students (e.g., Lu & Wang 2020; Li & Pu 2021). To appropriately include lateral entrainment process in models, future researches are recommended to focus on investigating the dynamic aspect that determines the actual fraction of the moat air entrained into eyewall and rainbands, quantifying the lateral entrainment velocity using observations and large-eddy simulations, and developing appropriate methods to explicitly include lateral entrainment buoyancy fluxes in the calculation of the buoyancy production of TKE in the TKE-based turbulent mixing schemes.

Open Research

Aircraft data, numerical simulation data, and Matlab codes for analyzing data used in this study can be accessed at http://vortex.ihrc.fiu.edu/download/Entrainment/.

Acknowledgments

This work is supported by NOAA/HFIP under the Grant NA18NWS4680057, NOAA/JTTI under the Grant NA22OAR4590177, and National Science Foundation under the Grants 2211307 and 2211308.

References

Crum, T. D., Stull, R. B., & Eloranta, E. W (1987), Coincident Lidar and Aircraft Observations of Entrainment into Thermals and Mixed Layers. J. *Climate App. Meteor*., 26, 774 – 788.

Deardorff, J. W. (1980), Cloud top entrainment instability. *J. Atmos. Sci*., 37, 131-147.

Li, X., & Pu, Z. (2021). Vertical eddy diffusivity parameterization based on a large-eddy simulation and its impact on prediction of hurricane landfall. Geophysical Research Letters, 48, e2020GL090703. https://doi.org/10.1029/2020GL090703.

Li, Y. B., Zhu, P., Gao, Z. Q., & Cheung, K (2022), Sensitivity of Large Eddy Simulations of Tropical Cyclone to Sub-Grid Scale Mixing Parameterization. *Atmospheric Research*. 265, 105922, https://doi.org/10.1016/j.atmosres.2021.

Lilly, D. K. (1968), Models of cloud-topped mixed layer under a strong inversion. *Quart. J. Roy. Meteor. Soc.*, 94, 292 – 837.

Lorsolo, S, Zhang, J. A., Marks, F. D., & Gamache, J. (2010), Estimation and mapping of hurricane turbulent energy using airborne Doppler measurements. *Mon. Wea. Rev.,* 138, 3656–3670, https://doi.org/10.1175/2010MWR3183.1.

Lu, X., & Wang, X. G., (2019), Improving hurricane analyses and predictions with TCI, IFEX field campaign observations, and CIMSS AMVs using the advanced hybrid data assimilation system for HWRF. Part I: What is missing to capture the rapid intensification of Hurricane Patricia (2015) when HWRF is already initialized with a more realistic analysis? *Mon. Wea. Rev*., 147 (4), 1351 – 1370.

Marks, F. D., Black, P. G., Montgomery, M. T., & Burpee, R. W. (2008), Structure of the eye and eyewall of Hurricane Hugo (1989). *Mon. Wea. Rev.,* 136, 1237–1259. https://doi.org/10.1175/2007MWR2073.1.

Randall, D. A. (1980), Conditional instability of the first kind upside down. *J. Atmos. Sci.*, 37, 125-130.

Shapiro, L. (1983), The asymmetric boundary-layer flow under a translating hurricane. *J. Atmos. Sci,* 40, 1984–1998.Smith, R. K, Montgomery, M. T., & Vogl, S. (2008), A critique of Emanuel's hurricane model and potential intensity theory. *Q. J. R. Meteorol. Soc.*, 134, 551–561.

Smith, R. K, & Montgomery, M. T. (2010), Hurricane boundary layer theory. *Q. J. R. Meteorol. Soc.*, 136, 1665–1670.

Stull, R. B., (1988), *An introduction to boundary-layer meteorology*. Kluwer: Dordrecht, The Netherlands, 670pp.

Zhang, J. A., R. F. Rogers, D. S. Nolan, & F. D. Marks, (2011), On the characteristic height scales of the hurricane boundary layer. Monthly Weather Review, 139, 2523-2535, https://doi.org/10.1175/MWR-D-10-05017.1.

Zhang, J. A., & Montgomery, M. T. (2012). Observational Estimates of the Horizontal Eddy Diffusivity and Mixing Length in the Low-Level Region of Intense Hurricanes, Journal of the Atmospheric Sciences, 69(4), 1306-1316. https://doi.org/10.1175/JAS-D-11-0180.1

Zhu, P., Tyner, B., Zhang, J. A., Aligo, E., Gopalakrishnan, S., Marks, F. D., Mehra, A., & Tallapragada, V. (2019), Role of eyewall and rainband in-cloud turbulent mixing in tropical cyclone intensification. *Atmospheric Chemistry and Physics,* 19, 14289–14310, https://doi.org/10.5194/acp-19-14289-2019.

Zhu, P., Hazelton, A., Zhang, Z., Marks, D. F., & Tallapragada, V. (2021). The Role of Eyewall Turbulent Transport in the Pathway to Intensification of Tropical Cyclones. *J. Geophy. Res. - Atmospheres*. 126(17), e2021JD034983, https://doi.org/10.1029/2021JD034983.